



Research Article

An analytical approach to design horns and boosters of ultrasonic welding machines



Amir Yazdian¹ · Mohammad Reza Karafi¹ 

Received: 4 December 2021 / Accepted: 25 April 2022

Published online: 13 May 2022

© The Author(s) 2022 [OPEN](#)

Abstract

This paper presents a new design approach for two main components of an ultrasonic plastic welding machine, booster and horn, based on an analytical model. The design procedure is developed due to the lack of a comprehensive and precise analytical model for rapid design and analysis of these components. The previous analytical models use the one-dimensional wave equation that causes significant errors in designing components with large lateral dimensions. Three-dimensional vibrations are considered for developing an analytical model using the apparent elasticity method. In this way, longitudinal frequency equations are coupled with radial frequency equations by mechanical coupling coefficients. Also, the damping of materials is taken into account. The model can be adapted to calculate the resonant length of the components or calculate the resonant frequency. To verify the model, the results are compared to a numerical simulation. The difference between analytical and numerical resonance frequency is less than 0.02%. Moreover, an experimental modal analysis is performed, which shows 0.9% error with analytical results.

Article highlights

- A new design approach for boosters and horns has been developed based on an analytical model.
- Three-dimensional vibrations are considered in the model using the apparent elasticity method.
- The accuracy of calculating resonant frequencies is more than one-dimensional design method.

Keywords Horn · Booster · Ultrasonic welding · Analytical model · Resonance frequency · Design

1 Introduction

Ultrasonic welding is a standard method for welding particular materials such as plastics. This welding method is based on propagating ultrasound waves along components and heating workpieces due to visco-elastic losses and the friction between surfaces. Ultrasonic horn and booster must be designed to have a longitudinal mode

shape in the desired working frequency. The resonant frequency can be altered by dimensional changes [1]. There are two general approaches to design ultrasonic horns and boosters: (i) traditional approach based on one-dimensional wave equation in the longitudinal direction (ii) finite element simulations [2]. Using finite element softwares is very common because of its simplicity, but designing dimensions with this method would be extremely

✉ Mohammad Reza Karafi, karafi@modares.ac.ir | ¹Faculty of Mechanical Engineering, Tarbiat Modares University, Tehran, Iran.



time-consuming. In most cases, the horns are designed conical, exponential, stepped, and cylindrical [3]. Nad et al. [4] examined various shapes of horns and presented the most optimal shape for the design of horns. Dang et al. [5] showed that the horn's vibrational amplitude with Bezier profile is more significant than other curves. Also, the results showed that this kind of horn is more durable due to less stress concentration and has a uniform amplitude of vibrations in its output surface. On the other hand, the stepped horn has the highest amplitude and suffers more stress concentration in the corners, which reduces its life dramatically. Singh et al. [6] compared stepped and exponential horns with two different materials using ANSYS software. Li et al. [7] modeled a horn according to spring-mass-damper interaction in one direction and two degree-of-freedom (DOF). The results showed a 0.1% difference between experiments and the proposed model for the resonance frequency. Wang and Lin [8] compared six different types of large cylindrical horns to reduce lateral vibrations utilizing COMSOL software. Also, they investigated the vibration uniformity of output surfaces of these horns. They stated that it is challenging to present an analytical solution for large-sized grooved horns because of their complex shapes. Carboni [9] explored the cause of cracking of corners and slots in two kinds of horns by FEM software. Kumar et al. [10] researched the necessity of considering slots on a horn's body and its effect on displacement uniformity of the output surface and its optimal location. Naseri et al. [11] designed a steel horn using FEM software for equal channel angular pressing (ECAP). Rani et al. [12] designed a horn with different materials and assessed the effect of temperature on the nodal plane experimentally and numerically. Yu et al. [13] modeled a horn using a one-dimensional wave equation. They approximated the length of two elements of the horn with constant cross-section by a 1D analytical model. However, they investigated the effect of temperature on the resonance frequency numerically using FEM software, and they showed that the resonance frequency decreases with the increasing temperature. Kumar and Prakasan [14] designed two different horns for joining metallic parts. They used the sound velocity through the horn for calculating the total length of the horn. Next, they calculated other dimensions using FEM software based on a methodology of trial and error that they had proposed for optimizing essential parameters.

Based on the literature survey, horn and booster were typically designed by FEM software. The presence of an analytical model is necessitated to investigate the effect of each parameter on the resonance frequency by a mathematical model. However, in some of these studies, it is mentioned that the use of a one-dimensional analytical model cannot be reliable and reasonable due to its

amount of error caused by the large lateral dimensions of horns.

In this paper, a design procedure is developed due to the lack of a comprehensive and precise analytical model for rapid design and analysis of these components. The previous analytical models use a one-dimensional wave equation that causes significant errors in designing components with large lateral dimensions. Nevertheless, the absence of a unanimous mathematical model for accurate design of these components feels [15]. On the other hand, the traditional approach for designing these parts is not accurate because it considers only one-dimensional vibration. Therefore, a 3D vibrational model should be provided to design these components precisely. The nodal plan location, mode shape, and resonance frequency can be obtained with this model. In this study, a comprehensive mathematical model based on the coupling of longitudinal and radial vibration is developed to calculate horn and booster dimensions, resonance frequency, mode shape, and magnifying factors. To begin with, the analytical model for boosters and horns are presented. Next, the designed horn and booster with the analytical model are analyzed with FEM software to verify the analytical model. Finally, experimental tests have been conducted to verify the result of the model.

2 Analytical modeling

2.1 Theory

Horns and boosters are usually made up of Ti or Al-7075-T6. These components consist of a solid, hollow cylinder, and exponential sections. When the diameter to length ratio of a component is less than one-quarter of a wavelength, a one-dimensional wave equation can be used to model the components analytically [16]. Nevertheless, in general, there are radial and circumferential displacements in these components that should be considered for a more realistic model, especially in the case of workpieces with large lateral dimensions and short lengths to reduce the amount of error [17]. A cylindrical 3D element is taken, and stresses are exerted on it, shown in Fig. 1.

Mechanical coupling coefficient (n), is defined as the ratio of longitudinal stress (σ_z) to lateral stress consist of radial (σ_r) and circumferential stress (σ_θ).

$$n = \frac{\sigma_z}{\sigma_r + \sigma_\theta} \quad (1)$$

The mechanical coupling coefficient is related to the geometry of the component, and it is usually a negative number. Radial and longitudinal displacement equations are coupled with this parameter.

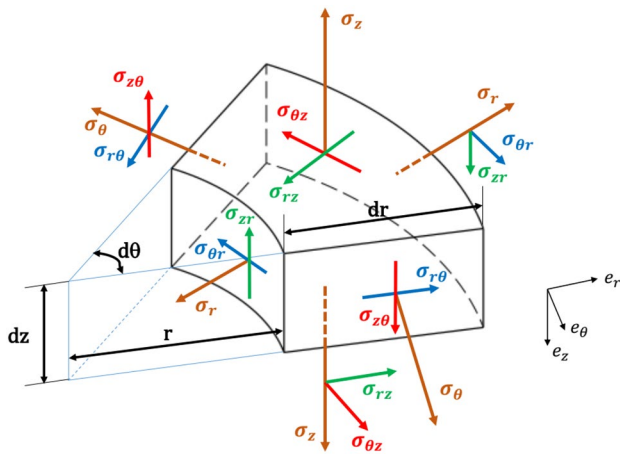


Fig. 1 The cylindrical element of components

The longitudinal displacement equation for a cylinder is obtained by solving the differential equation of displacement. u_z is the displacement and k_z is the apparent wave number in longitudinal direction.

$$\frac{\partial^2 u_z}{\partial z^2} + k_z^2 u_z = 0 \rightarrow u_z(z) = A \cos(k_z Z) + B \sin(k_z Z) \quad (2)$$

A and B in Eq. (2) remain unknown constants. The longitudinal displacement equation for an exponential part is:

$$u_z(z) = e^{-\beta z} \left(A \cos\left(\left[\sqrt{k_z^2 - \beta^2}\right]z\right) + B \sin\left(\left[\sqrt{k_z^2 - \beta^2}\right]z\right) \right) \quad (3)$$

Radial frequency equation for hollow and solid cylinders are obtained by solving the radial differential equation. u_r is the displacement and k_r is the apparent wave number in radial direction. J_0 is Bessel functions of the first kind and Y_0 is Bessel functions of the second kind.

$$\frac{\partial^2 u_r}{\partial r^2} + \frac{\partial u_r}{r \partial r} + \left(k_r^2 - \frac{1}{r^2}\right) u_r = 0 \rightarrow u_r(r) = C J_0(k_r r) + D Y_0(k_r r) \quad (4)$$

By applying boundary conditions for a hollow cylinder ($\sigma_{r=a} = 0, \sigma_{r=b} = 0$), radial frequency equation is obtained as follows.

$$\frac{k_r a J_0(k_r a) - \frac{(1-\nu-2\nu n)}{(1-\nu n)} J_1(k_r a)}{k_r b J_0(k_r b) - \frac{(1-\nu-2\nu n)}{(1-\nu n)} J_1(k_r b)} = \frac{k_r a Y_0(k_r a) - \frac{(1-\nu-2\nu n)}{(1-\nu n)} Y_1(k_r a)}{k_r b Y_0(k_r b) - \frac{(1-\nu-2\nu n)}{(1-\nu n)} Y_1(k_r b)} \quad (5)$$

a and b are the external and internal radius of the hollow cylinder respectively and ν is Poisson's ratio.

By applying boundary conditions ($u_{r=0} = 0, \sigma_{r=a} = 0$), radial frequency equation for a solid cylinder (Fig. 2a) is obtained:

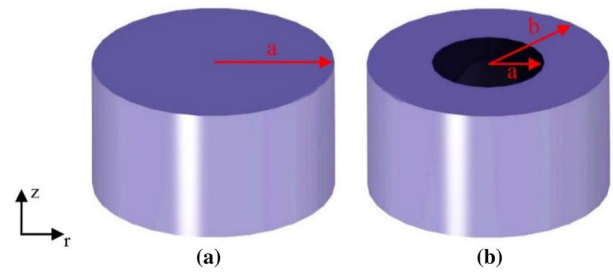


Fig. 2 a Solid and b hollow cylinder

$$a k_r J_0(k_r a) - \left[\frac{(1-\nu-2\nu n)}{(1-\nu n)} \right] J_1(k_r a) = 0 \quad (6)$$

The following assumptions are considered for the analytical model:

- (1) The vibration mode does not change in the wave propagation along the components.
- (2) Shear stresses and strains are ignored.
- (3) The waves inside the components are assumed sinusoidal.
- (4) The diameter change in the components is far from the critical values, so the effect of chamfers and fillets are ignored.
- (5) The acoustic impedance of air is ignored, so the horn or booster that works in the air is called "unloaded," and its stress is considered zero.
- (6) The machined surfaces for the wrench seat on the booster and horn are ignored.
- (7) The booster and horn's torsional and bending mode shapes are ignored.
- (8) The effect of the screw that connects the booster and horn is ignored.
- (9) Wave differential equations are considered in the radial and longitudinal directions.
- (10) Differential equations in longitudinal and radial directions are related to each other by the mechanical coupling coefficient.
- (11) To write the radial frequency equation of the exponential segments of the booster and horn, the mean radius of these segments is used.

2.2 Analytical model of booster and horn

Figure 2 presents the booster. The booster is divided into eight segments, including hollow and solid cylinder and exponential part. The geometrical shape of the booster increases the amplitude of oscillations.

According to Eqs. (5) and (6), the radial frequency equations of segments 1 to 8 are as follows [18].

$$\frac{k_{ri}a_i J_0(k_{ri}a_i) - \frac{1-v_i-2v_i n_i}{1-v_i n_i} J_1(k_{ri}a_i)}{k_{ri}b_i J_0(k_{ri}b_i) - \frac{1-v_i-2v_i n_i}{1-v_i n_i} J_1(k_{ri}b_i)} - \frac{k_{ri}a_i Y_0(k_{ri}a_i) - \frac{1-v_i-2v_i n_i}{1-v_i n_i} Y_1(k_{ri}a_i)}{k_{ri}b_i Y_0(k_{ri}b_i) - \frac{1-v_i-2v_i n_i}{1-v_i n_i} Y_1(k_{ri}b_i)} = 0, \quad i = 1, 2, 8 \tag{7}$$

$$k_{ri}a_i J_0(k_{ri}a_i) - \frac{1-v_i-2v_i n_i}{1-v_i n_i} J_1(k_{ri}a_i) = 0, \quad i = 3, 4, 5, 6, 7 \tag{8}$$

To obtain the longitudinal frequency equation, according to Eqs. (2) and (3), the displacement equations for each segment are written, then boundary conditions are applied (Fig. 3). The longitudinal displacement equations of segments 1 to 8 are as follows:

$$u_8(z_8) = A \cos(k_8 z_8) + B \sin(k_8 z_8) \tag{9}$$

$$u_7(z_7) = C \cos(k_7 z_7) + D \sin(k_7 z_7) \tag{10}$$

$$u_6(z_6) = e^{-\beta_2 z_6} \left(E \cos\left(\left[\sqrt{k_6^2 - \beta_2^2}\right] z_6\right) + F \sin\left(\left[\sqrt{k_6^2 - \beta_2^2}\right] z_6\right) \right) \tag{11}$$

$$u_5(z_5) = G \cos(k_5 z_5) + H \sin(k_5 z_5) \tag{12}$$

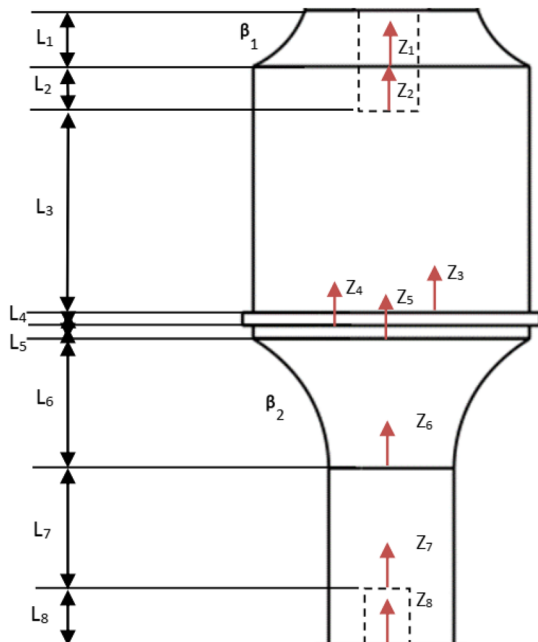
$$u_4(z_4) = I \cos(k_4 z_4) + J \sin(k_4 z_4) \tag{13}$$

$$u_3(z_3) = K \cos(k_3 z_3) + L \sin(k_3 z_3) \tag{14}$$

$$u_2(z_2) = M \cos(k_2 z_2) + N \sin(k_2 z_2) \tag{15}$$

$$u_1(z_1) = e^{\beta_1 z_1} \left(O \cos\left(\left[\sqrt{k_1^2 - \beta_1^2}\right] z_1\right) + P \sin\left(\left[\sqrt{k_1^2 - \beta_1^2}\right] z_1\right) \right) \tag{16}$$

By considering the assumptions and using boundary conditions in longitudinal equations, Eq. (17) has been obtained. [X] is the unknown coefficient of A, B, C ... The condition for the existence of a solution is that the determinant of the coefficient matrix should be equal to zero. The longitudinal frequency equation is obtained by this condition. Next, with solving radial frequency equations and longitudinal frequency equation, the resonance frequency of the booster and the mechanical coupling coefficient of each segment are calculated.



B.C.1: $F_1(L_1) = A_1 E_1 \frac{\partial u_1}{\partial z_1}(Z_1 = L_1) = 0$

B.C.2: $F_2(L_2) = F_1(0)$, **B.C.3:** $u_2(L_2) = u_1(0)$

B.C.4: $F_3(L_3) = F_2(0)$, **B.C.5:** $u_3(L_3) = u_2(0)$

B.C.6: $F_4(L_4) = F_3(0)$, **B.C.7:** $u_4(L_4) = u_3(0)$

B.C.8: $F_5(L_5) = F_4(0)$, **B.C.9:** $u_8(L_5) = u_4(0)$

B.C.10: $F_6(L_6) = F_5(0)$, **B.C.11:** $u_6(L_6) = u_5(0)$

B.C.12: $F_7(L_7) = F_6(0)$, **B.C.13:** $u_7(L_7) = u_6(0)$

B.C.14: $F_8(L_8) = F_7(0)$, **B.C.15:** $u_8(L_8) = u_7(0)$

B.C.16: $F_8(0) = A_8 E_8 \frac{\partial u_8}{\partial z_8}(Z_8 = 0) = 0$

Fig. 3 The booster elements and boundary conditions

Table 4 Horn’s dimensions

| Element number | Length (mm) | Inner radius (mm) | Outer radius (mm) |
|----------------|-------------|-------------------|-------------------|
| First | 53.7 | 0 | 12.5 |
| Second | 15 | 0 | 17.5 |
| Third | 60 | 0 | 17.5 |

Table 5 The resonant frequency and mechanical coupling coefficients

| | |
|---|-----------|
| Longitudinal resonance frequency | 19,943 Hz |
| Mechanical coupling coefficient of first element | −42.74 |
| Mechanical coupling coefficient of second element | −30.97 |
| Mechanical coupling coefficient of third element | −27.02 |

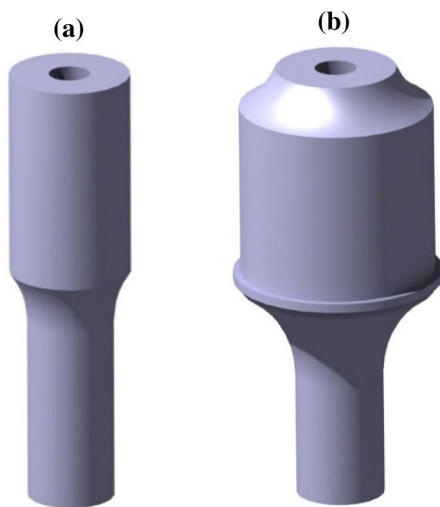


Fig. 5 **a** Horn and **b** Booster modeled in CATIA

The value of each alpha is in the appendix. The non-linear system of equations for the booster is achieved by one longitudinal and eight radial frequency equations. All dimensions and material properties are given in the equations. The resonance frequency and mechanical coupling coefficients of each section remain unknown parameters. Table 1 shows the dimensions of the booster, and Table 2 shows AL 7075-T6 mechanical characteristics.

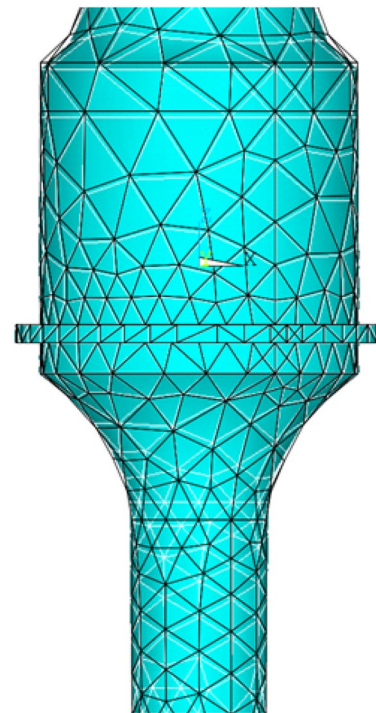


Fig. 6 Generated mesh for booster

The resonant frequency of the transducer has been measured as 19,943 Hz. The resonant frequency of all components should be matched in order to prevent loss and have a completely longitudinal mode shape. Considering the resonant frequency of the transducer, the results of solving the system of equations using MATLAB are reported in Table 3.

Figure 4 shows the horn. The horn is divided into three segments, including solid cylinder and exponential part.

The radial frequency equations of segments 1 to 3 are as follows.

$$k_i a_i J_0(k_i a_i) - \frac{1 - \nu_i - 2\nu_i n_i}{1 - \nu_i n_i} J_1(k_i a_i) = 0, \quad i = 1, 2, 3 \tag{19}$$

The displacement equations for each element are as follows.

$$u_1(z_1) = A \cos(k_1 z_1) + B \sin(k_1 z_1) \tag{20}$$

$$u_2(z_2) = e^{-\beta_1 z_2} \left(C \cos\left(\left[\sqrt{k_2^2 - \beta_1^2}\right] z_2\right) + D \sin\left(\left[\sqrt{k_2^2 - \beta_1^2}\right] z_2\right) \right) \tag{21}$$

Fig. 7 Booster's mode shape of the first longitudinal resonance frequency at 19,945.7 Hz

NODAL SOLUTION
 STEP=1
 SUB =12
 FREQ=19945.7
 USUM (AVG)
 RSYS=0
 DMX =3.65228
 SMN =.247835
 SMX =3.65228

MAY 12 2019
 23:14:03

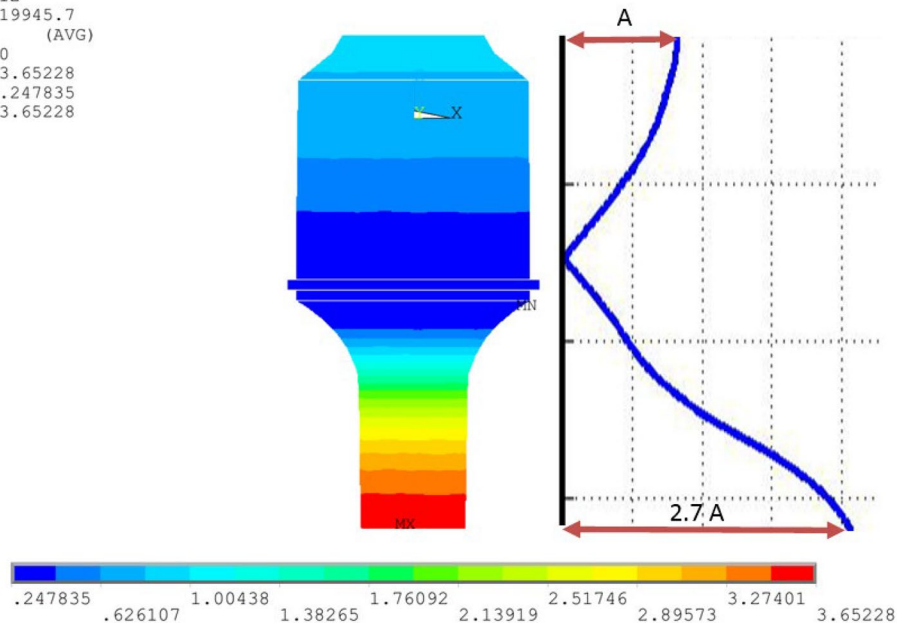
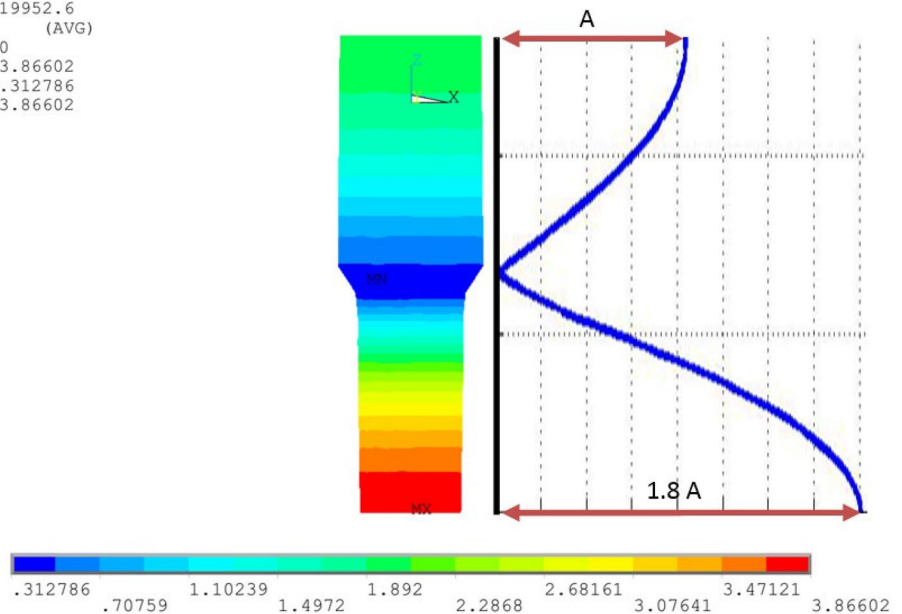


Fig. 8 Horn's mode shape of the first longitudinal resonance frequency of 19,952.6 Hz

NODAL SOLUTION
 STEP=1
 SUB =12
 FREQ=19952.6
 USUM (AVG)
 RSYS=0
 DMX =3.86602
 SMN =.312786
 SMX =3.86602

MAY 5 2019
 19:21:17



$$u_3(z_3) = E \cos(k_3 z_3) + F \sin(k_3 z_3) \tag{22}$$

By placing the boundary conditions into displacement equations, the longitudinal matrix equation of the horn is derived.

$$\begin{bmatrix} 0 & \alpha_1 & 0 & 0 & 0 & 0 \\ \alpha_2 & \alpha_3 & \alpha_4 & 0 & 0 & 0 \\ \alpha_5 & \alpha_6 & \alpha_7 & \alpha_8 & 0 & 0 \\ 0 & 0 & \alpha_9 & \alpha_{10} & \alpha_{11} & 0 \\ 0 & 0 & \alpha_{12} & \alpha_{13} & 0 & \alpha_{14} \\ 0 & 0 & 0 & 0 & \alpha_{15} & \alpha_{16} \end{bmatrix} \begin{bmatrix} A \\ B \\ C \\ D \\ E \\ F \end{bmatrix} = \begin{bmatrix} 0 \\ 0 \\ 0 \\ 0 \\ 0 \\ 0 \end{bmatrix} \tag{23}$$



Fig. 9 Fabricated booster and horn

The non-linear system of equations for horn is achieved by one longitudinal and three radial frequency equations in the same way as the booster. Table 4 shows the dimensions of the horn and Table 5 reports the results of solving the system of equations using MATLAB.

3 Numerical modeling

ANSYS software is used for numerical analysis. For this purpose, the booster and horn are modeled in the CATIA software (Fig. 5) with the same dimensions in the analytical

analysis. Subsequently they are imported into the ANSYS software for modal analysis. In the numerical analysis, the longitudinal resonance frequency, mode shape, and magnification factor of the horn and booster are computed. Also, the results are compared with analytical ones. The mechanical characteristics are demonstrated in Table 2.

Figure 6 shows generated mesh for the booster. The free mesh type is chosen for this study. The mesh type is triangular, and the number of Nodes is 6481.

The booster's modal analysis results are shown in Fig. 7. The first longitudinal resonance frequency is 19945 Hz, which shows a 0.01% error with the analytical result (19,943 Hz). On the other hand, the magnification factor of the component is 3.6, which shows a 25% error with the analytical result (2.7). Moreover, according to Fig. 7 the nodal plane is placed at a proper distance on the flange. The displacements should be minimum on the flange to cause less effect on the resonance frequency of the booster.

Figure 8 shows the horn's modal analysis results. The first longitudinal resonance frequency is 19952 Hz, which shows 0.01% error with the analytical result (19,943 Hz) and the magnification factor of the horn is 1.8.

4 Fabrication and experimental tests

The booster and the horn which is designed analytically, are fabricated for the sake of experimental tests. The longitudinal resonance frequency is calculated by modal hammer test for each component. Figure 9. shows fabricated booster and horn. The results of this test show longitudinal resonance frequency of booster and horn is 20110 Hz and 20,137 Hz respectively, which have 0.83% and 0.96% error with analytical results and 0.82% and 0.91% with numerical results.

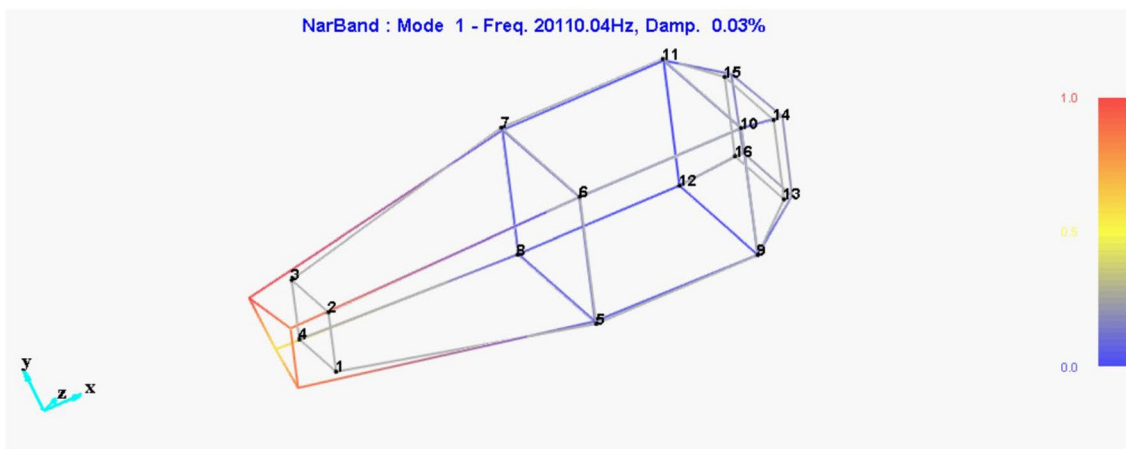


Fig. 10 Booster's mode shape

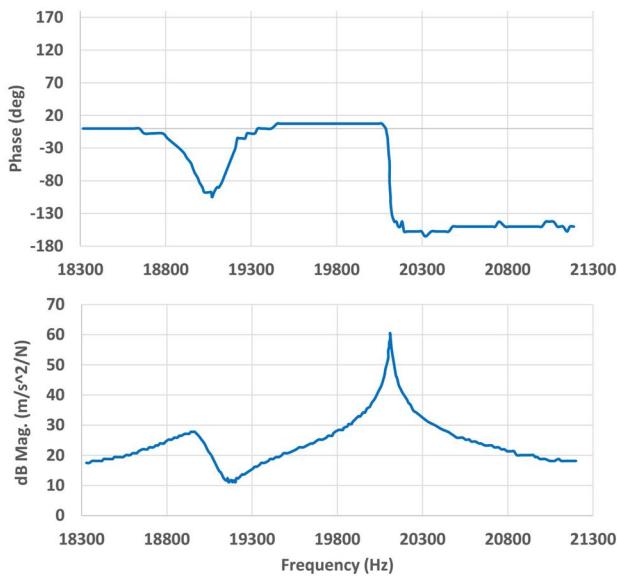


Fig. 11 Booster's frequency response function (FRF) diagram

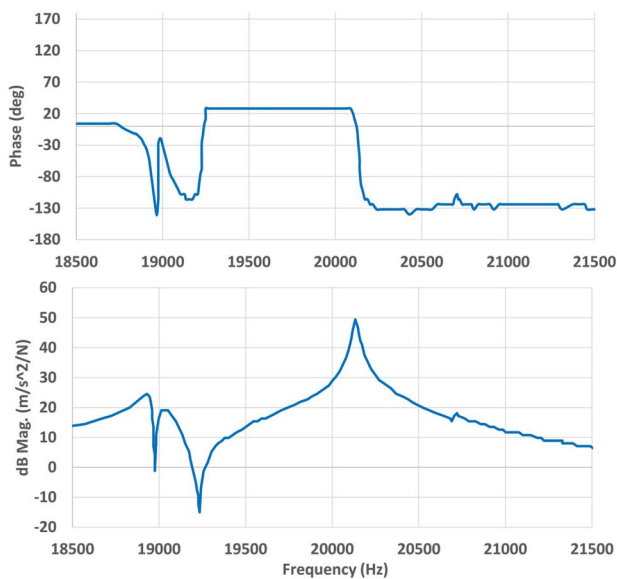


Fig. 12 Horn's frequency response function (FRF) diagram

Figure 10 shows the 3-D mode shape of the booster.

Also, frequency response function (FRF) diagrams of these components have been shown in Figs. 11 and 12. The magnification factor of the component is 3, which shows 16.66% and 10% errors with numerical and analytical results respectively.

Table 6 shows a summary of results and comparisons.

Table 7 shows the difference between 1 and 3D analytical model results. The calculated resonance frequency of the horn and the booster using a 3D analytical model is more accurate than a 1D model. The reason is that the lateral vibration is taken into account in a 3D analytical model.

5 Discussion

This study introduced a new approach to designing ultrasonic horns and boosters using a three-dimensional analytical model. The results were compared with numerical simulations and experimental tests. As shown in Table 6 the measured resonance frequency is quite close to its expected amount in the experimental test. According to Table 7 the accuracy of the 3D analytical model is higher than the 1D model due to consideration of lateral vibrations. Also, the magnification factor of the booster was calculated using the 3D analytical model.

Designing ultrasonic boosters and horns is time-consuming and requires trial and error to tune them for a special application, the 3D analytical model eliminates the trial and error process and makes these components easy to modify and optimize.

6 Conclusion

A new analytical design procedure was developed for designing horns and boosters of the ultrasonic plastic welding machine. The design procedure considers the longitudinal and lateral vibration of the component. The error of the conventional 1D vibrational equation is sharply decreased by using the new design procedure. The results of the analytical design were compared with the numerical results and experimental tests. Also, 1D and 3D

Table 6 Measured resonance frequency of the booster and the horn, magnification factor of the booster and comparisons between the results

| | Unit | Analytical | Numerical | Experimental | Analytical and numerical error (%) | Analytical and experimental error (%) | Numerical and experimental error (%) |
|--------------------------------|------|------------|-----------|--------------|------------------------------------|---------------------------------------|--------------------------------------|
| Booster's resonance frequency | Hz | 19,943 | 19,946 | 20,110 | 0.01 | 0.83 | 0.82 |
| Horn's resonance frequency | Hz | 19,943 | 19,953 | 20,137 | 0.01 | 0.96 | 0.91 |
| Booster's magnification factor | - | 2.7 | 3.6 | 3 | 25 | 10 | 16.66 |

Table 7 1D and 3D analytical comparisons

| Analytical | Unit | 3D | 1D | 1D and 3D analytical error (%) |
|-------------------------------|------|--------|--------|--------------------------------|
| Booster's resonance frequency | Hz | 19,943 | 19,531 | 2.07 |
| Horn's resonance frequency | Hz | 19,943 | 19,157 | 3.94 |

analytical models were compared and showed that the 3D analytical model is more accurate. The 3D analytical model was more accurate than the 1D model. To sum up, the following results can be drawn from this study:

1. The proposed 3D analytical model can eliminate or reduce trial and error steps for designing each component using FEM software which remains a time-consuming process for designers.
2. Designed components with this method were more accurate than previous analytical models.
3. A reliable mathematical model was proposed to investigate the effect of different length, material properties and radius of elements on the resonant frequency, mode shape, and magnification factor of ultrasonic boosters and horns for the first time.

Moreover, the proposed 3D analytical model can be developed to calculate the frequency response of the complete vibrating set of ultrasonic plastic welding including, transducer, booster, and horn. Also, using the proposed mathematical model, different optimizations can be conducted in order to increase the efficiency of these components.

Funding The authors declare that no funds, grants, or other support were received during the preparation of this manuscript.

Declarations

Conflict of interest The authors have no relevant financial or non-financial interests to disclose.

Open Access This article is licensed under a Creative Commons Attribution 4.0 International License, which permits use, sharing, adaptation, distribution and reproduction in any medium or format, as long as you give appropriate credit to the original author(s) and the source, provide a link to the Creative Commons licence, and indicate if changes were made. The images or other third party material in this article are included in the article's Creative Commons licence, unless indicated otherwise in a credit line to the material. If material is not included in the article's Creative Commons licence and your intended use is not permitted by statutory regulation or exceeds the permitted use, you will need to obtain permission directly from the copyright holder. To view a copy of this licence, visit <http://creativecommons.org/licenses/by/4.0/>

Appendix

The amount of each alpha in booster's matrix equation:

$$\alpha 1 = k_1$$

$$\alpha 2 = \cos(k_1 L_1)$$

$$\alpha 3 = \sin(k_1 L_1)$$

$$\alpha 4 = -1$$

$$\alpha 5 = -A_1 E_1 k_1 \sin(k_1 L_1)$$

$$\alpha 6 = A_1 E_1 k_1 \cos(k_1 L_1)$$

$$\alpha 7 = A_{23} E_2 \beta_1$$

$$\alpha 8 = -A_{23} E_2 \sqrt{k_2^2 - \beta_1^2}$$

$$\alpha 9 = e^{-\beta_1 L_2} \cos\left(\sqrt{k_2^2 - \beta_1^2} L_2\right)$$

$$\alpha 10 = e^{-\beta_1 L_2} \sin\left(\sqrt{k_2^2 - \beta_1^2} L_2\right)$$

$$\alpha 11 = -1$$

$$\alpha 12 = A_{23} E_2 e^{-\beta_1 L_2} \left(-\beta_1 \cos\left(\sqrt{k_2^2 - \beta_1^2} L_2\right) - \sqrt{k_2^2 - \beta_1^2} \sin\left(\sqrt{k_2^2 - \beta_1^2} L_2\right)\right)$$

$$\alpha 13 = A_{23} E_2 e^{-\beta_1 L_2} \left(-\beta_1 \sin\left(\sqrt{k_2^2 - \beta_1^2} L_2\right) + \sqrt{k_2^2 - \beta_1^2} \cos\left(\sqrt{k_2^2 - \beta_1^2} L_2\right)\right)$$

$$\alpha 14 = -A_3 E_3 k_3$$

$$\alpha 15 = -A_3 E_3 k_3 \cos(k_3 L_3)$$

$$\alpha 16 = A_3 E_3 k_3 \sin(k_3 L_3)$$

$$\alpha 17 = -1$$

$$\alpha 18 = -A_3 E_3 k_3 \sin(k_3 L_3)$$

$$\alpha 19 = A_3 E_3 k_3 \cos(k_3 L_3)$$

$$\alpha 20 = -A_4 E_4 k_4$$

$$\alpha 21 = \cos(k_4 L_4)$$

$$\alpha 22 = \sin(k_4 L_4)$$

$$\alpha 23 = -1$$

$$\alpha 24 = -A_4 E_4 k_4 \sin(k_4 L_4)$$

$$\alpha 25 = A_4 E_4 k_4 \cos(k_4 L_4)$$

$$\alpha 26 = A_{55} E_5 \beta_2$$

$$\alpha 27 = -A_{55} E_5 \sqrt{k_5^2 - \beta_2^2}$$

$$\alpha 28 = e^{-\beta_2 L_5} \cos\left(\sqrt{k_5^2 - \beta_2^2} L_5\right)$$

$$\alpha 29 = e^{-\beta_2 L_5} \sin\left(\sqrt{k_5^2 - \beta_2^2} L_5\right)$$

$$\alpha 30 = -1$$

$$\alpha_{31} = A_5 E_5 e^{-\beta_2 L_5} \left(-\beta_2 \cos \left(\sqrt{k_5^2 - \beta_2^2} L_5 \right) - \sqrt{k_5^2 - \beta_2^2} \sin \left(\sqrt{k_5^2 - \beta_2^2} L_5 \right) \right)$$

$$\alpha_{32} = A_5 E_5 e^{-\beta_2 L_5} \left(-\beta_2 \sin \left(\sqrt{k_5^2 - \beta_2^2} L_5 \right) + \sqrt{k_5^2 - \beta_2^2} \cos \left(\sqrt{k_5^2 - \beta_2^2} L_5 \right) \right)$$

$$\alpha_{33} = -A_6 E_6 k_6$$

$$\alpha_{34} = \cos(k_6 L_6)$$

$$\alpha_{35} = \sin(k_6 L_6)$$

$$\alpha_{36} = -1$$

$$\alpha_{37} = -A_6 E_6 k_6 \sin(k_6 L_6)$$

$$\alpha_{38} = A_6 E_6 k_6 \cos(k_6 L_6)$$

$$\alpha_{39} = -A_7 E_7 k_7$$

$$\alpha_{40} = \cos(k_7 L_7)$$

$$\alpha_{41} = \sin(k_7 L_7)$$

$$\alpha_{42} = -1$$

$$\alpha_{43} = -A_7 E_7 k_7 \sin(k_7 L_7)$$

$$\alpha_{44} = A_7 E_7 k_7 \cos(k_7 L_7)$$

$$\alpha_{45} = -A_8 E_8 k_8$$

$$\alpha_{46} = \cos(k_8 L_8)$$

$$\alpha_{47} = \sin(k_8 L_8)$$

The amount of each alpha in horn's matrix equation:

$$\alpha_1 = k_1$$

$$\alpha_2 = \cos(k_1 L_1)$$

$$\alpha_3 = \sin(k_1 L_1)$$

$$\alpha_4 = -1$$

$$\alpha_5 = -A_1 E_1 k_1 \sin(k_1 L_1)$$

$$\alpha_6 = A_1 E_1 k_1 \cos(k_1 L_1)$$

$$\alpha_7 = A_2 E_2 \beta_1$$

$$\alpha_8 = -A_2 E_2 \sqrt{k_2^2 - \beta_1^2}$$

$$\alpha_9 = e^{-\beta_1 L_2} \cos \left(\sqrt{k_2^2 - \beta_1^2} L_2 \right)$$

$$\alpha_{10} = e^{-\beta_1 L_2} \sin \left(\sqrt{k_2^2 - \beta_1^2} L_2 \right)$$

$$\alpha_{11} = -1$$

$$\alpha_{12} = A_2 E_2 e^{-\beta_1 L_2} \left(-\beta_1 \cos \left(\sqrt{k_2^2 - \beta_1^2} L_2 \right) - \sqrt{k_2^2 - \beta_1^2} \sin \left(\sqrt{k_2^2 - \beta_1^2} L_2 \right) \right)$$

$$\alpha_{13} = A_2 E_2 e^{-\beta_1 L_2} \left(-\beta_1 \sin \left(\sqrt{k_2^2 - \beta_1^2} L_2 \right) + \sqrt{k_2^2 - \beta_1^2} \cos \left(\sqrt{k_2^2 - \beta_1^2} L_2 \right) \right)$$

$$\alpha_{14} = -A_3 E_3 k_3$$

$$\alpha_{15} = -A_3 E_3 k_3 \cos(k_3 L_3)$$

$$\alpha_{16} = A_3 E_3 k_3 \sin(k_3 L_3)$$

References

- Shu KM, Hsieh WH, Yen HS (2013) Design and analysis of acoustic horns for ultrasonic machining. *Appl Mech Mater* 284–287:662–666. <https://doi.org/10.4028/www.scientific.net/amm.284-287.662>

- Davim JP (2013) *Nontraditional machining processes: research advances*. Springer, London
- Nguyen L, Tsai Y, Hsieh Y, Hung C (2016) Finite element analysis of an ultrasonic vibration device at high temperatures. *Chin Mach Eng* 37:193–200
- Nad' M (2010) Ultrasonic horn design for ultrasonic machining technologies. *Appl Comput Mech* 4:79–88
- Wang D-A, Nguyen H-D (2014) A planar Bézier profiled horn for reducing penetration force in ultrasonic cutting. *Ultrasonics* 54(1):375–384. <https://doi.org/10.1016/j.ultras.2013.05.002>
- Singh DP, Mishra S, Porwal RK (2019) Modal analysis of ultrasonic horn using finite element method. *Mater Today Proc* 18(7):3617–3623. <https://doi.org/10.1016/j.matpr.2019.07.293>
- Li X, Harkness P, Worrall K, Timoney R, Lucas M (2017) A parametric study for the design of an optimized ultrasonic percussive planetary drill tool. *IEEE Trans Ultrason Ferroelectr Freq Control* 64(3):577–589. <https://doi.org/10.1109/TUFFC.2016.2633319>
- Wang S, Lin S (2019) Optimization on ultrasonic plastic welding system based on two-dimensional photonic crystal. *Ultrasonics*. <https://doi.org/10.1016/j.ultras.2019.105954>
- Carboni M (2014) Failure analysis of two aluminium alloy sonotrodes for ultrasonic plastic welding. *Int J Fatigue* 60:110–120. <https://doi.org/10.1016/j.ijfatigue.2013.05.013>
- Kumar RD, Rani MR, Elangovan S (2014) Design and analysis of slotted horn for ultrasonic plastic welding. *Appl Mech Mater* 592–594:859–863. <https://doi.org/10.4028/www.scientific.net/amm.592-594.859>
- Naseri R, Koohkan K, Ebrahim M, Djavanroodi F, Ahmadian H (2017) Horn design for ultrasonic vibration-aided equal channel angular pressing. *Int J Adv Manuf Technol* 90:1727–1734. <https://doi.org/10.1007/s00170-016-9517-0>
- Roopa Rani M, Prakasan K, Rudramoorthy R (2015) Studies on thermo-elastic heating of horns used in ultrasonic plastic welding. *Ultrasonics* 55:123–132. <https://doi.org/10.1016/j.ultras.2014.07.005>
- Yu J, Luo H, Nguyen TV, Huang L, Liu B, Zhang Y (2020) Eigenfrequency characterization and tuning of Ti-6Al-4V ultrasonic horn at high temperatures for glass molding. *Ultrasonics* 101:106002. <https://doi.org/10.1016/j.ultras.2019.106002>
- Pradeep Kumar J, Prakasan K (2018) Acoustic horn design for joining metallic wire with flat metallic sheet by ultrasonic vibrations. *J Vibroengineering* 20(7):2758–2770. <https://doi.org/10.21595/jve.2018.19648>
- Roopa Rani M, Rudramoorthy R (2013) Computational modeling and experimental studies of the dynamic performance of ultrasonic horn profiles used in plastic welding. *Ultrasonics* 53:763–772. <https://doi.org/10.1016/j.ultras.2012.11.003>
- O'Shea K (1991) Enhanced vibration control of ultrasonic tooling using finite element analysis. *Vib Anal-Comput ASME* 37:259–265
- Karafi M, Kamali S (2021) A continuum electro-mechanical model of ultrasonic Langevin transducers to study its frequency response. *Appl Math Model* 92:44–62. <https://doi.org/10.1016/j.apm.2020.11.006>
- Mori E, Yamakoshi K (1978) Coupled vibration of a cylindrical shell for radiating high intensity ultrasound. *Ultrasonics* 16(2):81–83. [https://doi.org/10.1016/0041-624X\(78\)90094-X](https://doi.org/10.1016/0041-624X(78)90094-X)
- Abdullah A, Malaki M (2013) On the damping of ultrasonic transducers' components. *Aerosp Sci Technol* 28(1):31–39. <https://doi.org/10.1016/j.ast.2012.10.002>

Publisher's Note Springer Nature remains neutral with regard to jurisdictional claims in published maps and institutional affiliations.